JCI The Journal of Clinical Investigation

Complement and inflammasome overactivation mediates paroxysmal nocturnal hemoglobinuria with autoinflammation

Britta Höchsmann, … , Peter M. Krawitz, Taroh Kinoshita

J Clin Invest. 2019. https://doi.org/10.1172/JCI123501.

Research In-Press Preview Hematology Inflammation

Graphical abstract

Title

Complement and inflammasome overactivation mediates paroxysmal nocturnal hemoglobinuria with autoinflammation

Authors

Britta Höchsmann[1+], Yoshiko Murakami[2,3+], Makiko Osato[2,4+], Alexej Knaus[5], Michi Kawamoto[6], Norimitsu Inoue[7], Tetsuya Hirata[2], Shogo Murata[2,8], Markus Anliker[1], Thomas Eggerman[9], Marten Jäger[10], Ricarda Floettmann[10], Alexander Höllein[11], Sho Murase[6], Yasutaka Ueda[4], Jun-ichi Nishimura[4], Yuzuru Kanakura[4], Nobuo Kohara[6], Hubert Schrezenmeier[1*], Peter M. Krawitz[5*], and Taroh Kinoshita[2,3*].

Author Affiliation

[1] Institute of Transfusion Medicine, University of Ulm and Institute of Clinical Transfusion Medicine and Immunogenetics, German Red Cross Blood Transfusion Service and University Hospital Ulm, Ulm, Germany; [2] Research Institute for Microbial Diseases, Osaka University, Japan; [3] WPI Immunology Frontier Research Center, Osaka University, Japan; [4] Department of Hematology and Oncology, Graduate School of Medicine, Osaka University, Japan; [5] Institute for Genomic Statistics and Bioinformatics, Rheinische Friedrich-Wilhelms-Universität Bonn, Germany; [6] Department of Neurology, Kobe City Medical Center General Hospital, Japan; [7] Department of Tumor Immunology, Osaka International Cancer Institute, Japan; [8] Department of Hematology/Oncology, Wakayama Medical University, Japan; [9] Institute for Human Genetics, RWTH, Aachen, Germany; [10] Department of Medical Genetics, Charite Hospital, University of Berlin, Germany; [11] MLL Muenchner Leukaemielabor GmbH, Munich, Germany.

[+]Equally contributed authors; *equally contributed corresponding authors.

Corresponding Authors:

Taroh Kinoshita, PhD.
Yabumoto Department of Intractable Disease Research, Research Institute for Microbial Diseases, Osaka University, 3-1 Yamada-oka, Suita, Osaka 565-0871, Japan
tkinoshi@biken.osaka-u.ac.jp
tel +81-6-6879-8328
fax +81-6-6875-5233

Peter M. Krawitz, PhD.
Institute for Genomic Statistics and Bioinformatics, Rheinische Friedrich-Wilhelms-Universität, Sigmund-Freud-Str. 25, 53127 Bonn, Germany
pkrawitz@uni-bonn.de
+49-228-287-14799

Hubert Schrezenmeier, MD.
Institute of Transfusion Medicine, University of Ulm and Institute of Clinical Transfusion Medicine and Immunogenetics, German Red Cross Blood Transfusion Service and University Hospital Ulm, Helmholtzstrasse 10, 89081 Ulm, Germany
h.schrezenmeier@blutspende.de
tel +49-731-150-550
fax +49-731-150-500

Conflict-of-interest statements

HS: research supports to University of Ulm from Novartis and Alexion Pharmaceuticals. Other authors have declared that no conflict of interest exists.

Abstract

Patients with paroxysmal nocturnal hemoglobinuria (PNH) have a clonal population of blood cells deficient in glycosylphosphatidylinositol (GPI)-anchored proteins, resulting from a mutation in the X-linked gene *PIGA*. Here we report on a set of patients in whom PNH results instead from biallelic mutation of *PIGT* on chromosome 20. These PIGT-PNH patients have clinically typical PNH, but they have in addition prominent auto-inflammatory features, including recurrent attacks of aseptic meningitis. In all these patients we find a germ-line point mutation in one *PIGT* allele, whereas the other *PIGT* allele is removed by somatic deletion of a 20q region comprising maternally imprinted genes implicated in myeloproliferative syndromes. Unlike in PIGA-PNH cells, GPI is synthesized in PIGT-PNH cells and, since its attachment to proteins is blocked, free GPI is expressed on the cell surface. From studies of patients' leukocytes and of *PIGT*-knockout THP-1 cells we show that, through increased IL-1β secretion, activation of the lectin pathway of complement and generation of C5b-9 complexes, free GPI is the agent of auto-inflammation. Eculizumab treatment abrogates not only intravascular hemolysis, but also auto-inflammation. Thus, PIGT-PNH differs from PIGA-PNH both in the mechanism of clonal expansion and in clinical manifestations.

Introduction

Paroxysmal nocturnal hemoglobinuria (PNH) is an acquired hematopoietic stem cell (HSC) disorder characterized by complement-mediated hemolysis, thrombosis and bone marrow failure (1, 2). Affected cells harbor a somatic mutation in the *PIGA* gene, essential for the initial step in glycosylphosphatidylinositol (GPI) biosynthesis that occurs in the endoplasmic reticulum (ER)(Figure 1**A**(a)) (3). Loss of GPI biosynthesis results in the defective expression of GPI-anchored proteins (GPI-APs) including complement inhibitors CD59 and DAF/CD55 (Figure 1**A**(b)). The affected stem cells generate large numbers of abnormal blood cells after clonal expansion that occurs under bone marrow failure. The affected erythrocytes are defective in complement regulation and destroyed by the membrane attack complex (MAC or C5b-9) upon complement activation (1). Eculizumab, an anti-complement component 5 (C5) monoclonal antibody (mAb), has been used to prevent intravascular hemolysis and thrombosis (4, 5). Eculizumab binds to C5 and inhibits its activation and subsequent generation of C5b-9 complexes.

Among more than 20 genes involved in GPI biosynthesis and transfer to proteins, *PIGA* is X-linked whereas all others are autosomal (6). Because of X-linkage, one somatic mutation in *PIGA* causes GPI deficiency in both males and females (3). In contrast, two mutations are required for an autosomal gene, but the probability of somatic mutations in both alleles at the same locus is extremely low, which explains why GPI deficiency in most patients with PNH is caused by *PIGA* somatic mutations. Recently, we reported two patients with PNH whose GPI-AP deficiency was caused by germline and somatic mutations in the *PIGT* gene localized on chromosome 20q (7, 8). Both patients had a heterozygous germline loss-of-function mutation in *PIGT*, along with loss of the normal allele of *PIGT* by a deletion of 8 or 18 Mb occurring in HSCs (7, 8). PIGT, forming a GPI transamidase complex with PIGK, PIGS, PIGU and GPAA1, acts in the transfer of preassembled GPI to proteins in the ER (Figure 1**A**(a)) (9). In *PIGT*-defective cells, GPI is synthesized but is not transferred to precursor proteins,

resulting in GPI-AP deficiency on the cell surface (Figure 1**A**(c)). We showed recently that non-protein-linked, free GPI remaining in the ER of *PIGT*-defective Chinese hamster ovary (CHO) cells is transported to and displayed on the cell surface (Figure 1**A**(c)) (10).

Two reported PNH patients with PIGT defect suffered from recurrent inflammatory symptoms that are unusual in patients with PNH (7, 8). Here, we report two more patients with PNH who lost *PIGT* function via a similar genetic mechanism, and present insights into the expansion of *PIGT*-defective clones common among four patients. We also present integrated clinical characteristics of these four patients and show that *PIGT*-defective mononuclear leukocytes, but not *PIGA*-defective mononuclear leukocytes, secreted IL1β in response to inflammasome activators. Using a *PIGT*-knockout THP-1 cell model, we show that complement activation is enhanced on the surface of *PIGT*-defective cells leading to MAC-dependent elevated secretion of IL1β. Against this background, we propose a distinct disease entity, PIGT-PNH.

Results

Case Report

Japanese patient J1 (8) and German patients G1 (7), G2, and G3 were diagnosed with PNH at the ages of 68, 49, 65, and 66, respectively. The changes in PNH clone sizes in J1, G1 and G3 after PNH diagnosis are shown in Figure 1**B**. They were treated with eculizumab, which effectively prevented intravascular hemolysis. Percent PNH cells rapidly increased after commencement of eculizumab not only in erythrocytes but also in granulocytes (Figure 1**B**). We reported that in G1, direct Coombs test positive erythrocytes appeared after commencement of eculizumab treatment, suggesting extravascular hemolysis (7). Blood cell counts for G1 and G3 are shown in Figure S1**A**. Before the diagnosis of PNH, J1, G1 and G3 had suffered inflammatory symptoms including urticaria, arthralgia and fever from the ages of 30, 26, and 48, respectively (Table 1). Urticaria in J1 was associated with neutrophil infiltration (8) and that in G3 with a mixed inflammatory infiltrate (Figure 1**C**). J1 (8) and G3 suffered from recurrent aseptic meningitis characterized by an abundance of neutrophils in cerebrospinal fluid. Following the initiation of eculizumab treatment for hemolysis 3–5 years previously, J1 and G3 had not suffered any episodes of meningitis (Figure 1**D**). Urticaria and arthralgia were also ameliorated in all three by eculizumab treatment. G2 had severe arteriosclerosis, which might be related to autoinflammation (Table 1), however, whether G2 had autoinflammatory symptoms is unclear and could not be confirmed because the patient passed away.

Genetic basis of GPI-AP deficiency

Four patients did not have *PIGA* somatic mutations but had a germline mutation in one allele of *PIGT* located on chromosome 20q: J1, NM_015937 (8): c.250G>T; G1, c.1401-2A>G (7); G2, c.761_764delGAAA; and G3, c.197delA (Figure S2**A**). These cause E84X, exon 11 skipping, frameshift after G254, and frameshift after Y66, respectively. The functional activities of variant *PIGT* found in J1 and G1 were reported to be very low (7, 11). Variants in G2 and G3 causing frameshifts should also be severely

deleterious to PIGT function. In addition to the germline *PIGT* mutation, all four had in the other allele a somatic deletion of 8–18 Mb, which includes the entire *PIGT* gene (Figure S2**B**) (7, 8). Therefore, in contrast to GPI-AP deficiency caused by a single *PIGA* somatic mutation in PNH, GPI-AP deficiency in all four is caused by a combination of germline loss-of-function *PIGT* mutation and somatic loss of the whole of normal *PIGT* in hematopoietic stem cells (Figure 2**A**).

A possible mechanism of clonal expansion in PIGT-PNH

Deletion of chromosome 20q represents the most common chromosomal abnormality associated with myeloproliferative disorders. The deleted region of 8–18 Mb included a "myeloid common deleted region" (CDR) (12) (Figure 2**A**). A fraction (approximately 10%) of patients with myeloproliferative neoplasm (MPN) such as polycythemia vera commonly have a deletion of 2.7 Mb in chromosome 20q (12). Moreover, a fraction (approximately 4%) of patients with myelodysplastic syndrome (MDS) also have a deletion of 2.6 Mb in this region (12). The CDR region shared by MPN and MDS spanning approximately 1.9 Mb has been called "myeloid CDR" (Figure 2**B**) and its loss was shown to be causally related to clonal expansion of the affected myeloid cells in these $20q^-$ syndromes (13). In contrast to previous cytogenetic analysis on classical PNH cases that showed no aberrations in 20q (14, 15), one allele of the myeloid CDR was lost in PNH cells of all four patients (Figure S2**B**) (7, 8).

The tumor suppressor-like gene *L3MBTL1* and the kinase gene *SGK2* located within the myeloid CDR (Figure 2**A**,**B**) are expressed only in the paternal allele due to gene imprinting (16). It was shown that losses of active paternal alleles of these two genes had a causal relationship with clonal expansion of these $20q^-$ myeloid cells (13). *L3MBTL1* and *SGK2* transcripts were undetectable in GPI-AP-defective granulocytes from J1 and extremely low in whole blood cells from G1, whereas they were found in granulocytes from healthy individuals (Figure 2**C**). The transcripts of two unimprinted genes, *IFT52* and *MYBL2*, were detected in both GPI-AP-defective

granulocytes from J1 and normal granulocytes (Figure 2**C**, top). The results therefore indicate that the expression of *L3MBTL1* and *SGK2* is lost in GPI-AP-defective cells in J1 and G1.

The results shown in Figure 2**C** also indicate that the somatically deleted region in J1 and G1 included active *L3MBTL1* and *SGK2*, so it was in the paternal chromosome. Owing to mRNA from patients G2 and G3 not being available, we determined the methylation status of the *L3MBTL1* gene using DNA from blood leukocytes, among which the large majority of cells were of the PNH phenotype. *L3MBTL1* in G1 and G3 samples was hypermethylated (Figure 2**D** and Figure S3**A**), indicating that the myeloid CDR allele remaining in their PNH clones was imprinted. In contrast, the G2 sample was hypomethylated. It was reported that, in some MPN patients with myeloid CDR deletion, the remaining allele was hypomethylated; nevertheless, its transcription was suppressed (13). G2 might be in a similar situation, although it was not possible to draw a definitive conclusion on this by RT-PCR analysis as the patient had passed away. These results indicate that the loss of expressed myeloid CDR allele is associated with clonal expansion of *PIGT*-defective cells similar to 20q− MPN and MDS.

Appearance of free GPI on the surface of PIGT-defective cells

PIGA is required for the first step in GPI biosynthesis (17); therefore, no GPI intermediate is generated in *PIGA*-defective cells (Figure 1**A**(b)). *PIGT* is involved in the attachment of GPI to proteins. GPI is synthesized in the ER, but is not used as a protein anchor in *PIGT*-defective cells (Figure 1**A**(c)). We used T5 mAb that recognizes free GPI, but not protein-bound GPI, as a probe to characterize free GPI (Figure 3A: see Methods for epitope and other characteristics of this antibody)(18, 19). Using T5 mAb in western blotting and flow cytometry, we first compared *PIGT*-defective CHO cells with *PIGL*-defective CHO cells, in which an early GPI biosynthetic step is defective, like in *PIGA*-defective cells. T5 mAb revealed a strong band of free GPI at a position corresponding to approximately 10 kDa in lysates of *PIGT*-defective cells but not of *PIGL*-defective cells (Figure 3**B**). DAF and

CD59 were not detected in either mutant cell, confirming that un-GPI-anchored precursor proteins were degraded (Figure 3**B**) (20). T5 mAb stained the surface of *PIGT*-defective CHO cells but not *PIGL*-defective cells, confirming that free GPI transported to the cell surface is detectable by T5 mAb (Figure 3**C**).

We then analyzed blood cells from J1, G1, and G3, and from patients with PIGA-PNH by flow cytometry. All four patients had PNH-type blood cells defective in various GPI-APs (Figures 3**D**–**F** and S4**A**, **B**). Erythrocytes from J1, G1, and G3 contained 3%, 84%, and 60% PNH cells, respectively, and a sizable fraction of them (36%, 87%, and 87%, respectively) were stained by T5 mAb (Figure 3**D**). J1 had PNH cells in granulocytes (81%), monocytes (87%), and B-lymphocytes (54%), but not T-lymphocytes (<2%), as revealed by anti-CD59 and GPI-binding probe fluorescence-labeled nonlytic aerolysin (FLAER) (21). Affected monocytes and B-lymphocytes were strongly stained by T5 mAb, whereas affected granulocytes were weakly but clearly stained (Figures 3**E** and S4**B**). Normal populations in granulocytes, monocytes and B-lymphocytes were not stained by T5 mAb (Figure 3**E**). Similar results, showing strong T5 staining of affected monocytes and granulocytes, were obtained with leukocytes from G1 and G3 (Figure 3**F**). In contrast, PNH cells from PIGA-PNH patients and cells from healthy individuals were not positively stained by T5 mAb (Figure 3**E**, **F**). Small fractions of wild-type erythrocytes from J1, G1, and G3 (0.13%, 9.7%, and 9.5%, respectively) were positively stained by T5 mAb (Figure 3**D**). Free GPI might be transferred from PNH cells to wild-type erythrocytes in vivo (22, 23), although the exact mechanism involved needs to be clarified. Thus, the surface expression of the T5 mAb epitope is specific for *PIGT*-defective cells and T5 mAb is useful to diagnose PIGT-PNH. It was noted that FLAER, which is conveniently used to stain cell-surface GPI-APs and to determine the affected cells in patients with PNH (21, 24), did not stain PIGT-PNH cells. Aerolysin specifically binds to the GPI moiety of some but not all GPI-APs, and requires simultaneous association with N-glycan for high-affinity binding (25-27). Our results indicate that FLAER binds to protein-bound GPI but not to free GPI.

We next investigated whether GPI-AP-defective clone was present in the stage only with autoinflammation. After determining the break points causing the deletion of 18 Mb in J1 (Figure S5), we quantitatively analyzed blood DNA samples for the presence of the break. It was estimated that a relative level of the break in the sample taken in a stage with autoinflammation only (#1) was approximately 10% of a level in the sample taken one month after start of eculizumab therapy (#2), which contained 29% PNH cells (Figure 3G). Therefore, approximately 3% of total leukocytes obtained 4 months before the onset of recurrent hemolysis were GPI-AP-defective cells.

Inflammasome- and complement-mediated autoinflammation, a feature of PIGT-PNH

IL18 levels were elevated in serum samples taken from J1 before and after the commencement of eculizumab therapy (Table 2), suggesting that this phenomenon was not dependent upon C5 activation. Serum amyloid A was also elevated before eculizumab therapy, but was within the normal range after the commencement of eculizumab therapy (Table 2), suggesting that the elevation was dependent upon C5 activation. In G3, increased levels of soluble IL2 receptor and thymidine kinase before, but not after, the start of eculizumab therapy suggested autoinflammation (Table 2). Serum amyloid A (up to 10.5 μg/ml; normal range <5 μg/ml) was also elevated. Combination therapies of prednisolone with anakinra, an IL1 receptor antagonist, or canakinumab, a mAb against IL1β, were effective at reducing urticaria (but not arthralgia and meningitis episodes) of G3. In G1, the IL18 level was above the normal range during eculizumab therapy (195 pg/ml; normal range <150 pg/ml). These lines of evidence suggest that autoinflammatory symptoms are associated with inflammasome activation. We also measured IL18, serum amyloid A, and lactate dehydrogenase (LDH) in serum samples from four patients with PIGA-PNH who were not undergoing eculizumab therapy. The levels of IL18 (263–443 pg/ml; normal range <211 pg/ml) and serum amyloid A (5.0–8.3 μg/ml) were within or slightly higher than the

normal ranges, whereas LDH levels were markedly elevated (Table 2). These results suggest that autoinflammation is a feature of PIGT-PNH.

We next compared mononuclear cells from J1, patients with PIGA-PNH, and healthy donors for IL1β production upon stimulation by NLRP3-inflammasome activators (28). Cells from three PIGA-PNH patients secreted only very low levels of IL1β after stimulation by Pam_3CSK4 (TLR2 ligand) and ATP or monosodium urate (MSU) (Figure 4**A** right and 4**B**). In contrast, cells from J1 secreted 45–60 times as much IL1β and the levels were even higher than those from healthy control cells (Figure 4**A** left and 4**B**). A similar difference between PIGT- and PIGA-defective cells was seen upon stimulation by lipoteichoic acid (LTA: another TLR2 ligand) and ATP or MSU (Figure 4**B**). Low IL1β response of PIGA-defective cells was predicted because they lack CD14, a GPI-anchored co-receptor of TLRs. However, PIGT-defective cells also lacking CD14 showed a strong IL1β response. These results indicate that NLRP3 inflammasomes are easily activated and support the idea that the presence of non-protein-linked free GPI is associated with efficient activation of NLRP3 inflammasomes, contributing to autoinflammatory symptoms in PIGT-PNH.

To investigate the roles of complement in inflammasome activation in PIGT-PNH, we switched to a model cell system because patients' blood cells were easily damaged in vitro under conditions of complement activation. PIGTKO and PIGAKO cells were generated from human monocytic THP-1 cells (Figure S6**A**) and were differentiated to macrophages. They showed IL1β response comparable to those of authentic inflammasome activators (Figure S6**B**). To analyze the inflammasome response to activated complement, these THP-1-derived macrophages were stimulated with acidified serum (AS), which causes activation of the alternative complement pathway. PIGTKO and PIGAKO cells but not WT cells secreted IL1β (1221.8±91.6, 568.2±101 and 23.7±2.2 pg/ml for PIGTKO, PIGAKO, and WT cells, respectively) (Figure 5**A**). This result is consistent with impaired complement regulatory activities on PIGTKO and PIGAKO cells, and normal

complement regulatory activity on WT cells. PIGTKO cells secreted approximately twice as much IL1β as PIGAKO cells (p<0.01). However, IL1β production returned to near the WT cell level after the transfection of *PIGT* and *PIGA* cDNAs into PIGTKO and PIGAKO cells, respectively (Figure 5**B**). The levels of IL1β mRNA and protein were comparable in WT, PIGTKO, and PIGAKO cells (Figure S7**A** and S7**B**). Therefore, PIGT KO enhanced the secretion but not the generation of IL1β.

Heat inactivation of complement and the addition of anti-C5 mAb to AS almost completely inhibited IL1β secretion (Figure 5**A**). These results indicate that IL1β secretion requires the activation of C5 on PIGTKO and PIGAKO cells. The activation of C5 leads to two biologically active products, C5a and MAC (29). To address which of these is important for IL1β secretion, cells were treated with the C5aR antagonist W-54011 (30) or anti-C5aR mAb to inhibit the signal transduction through C5aR. WT, PIGTKO, and PIGAKO cells expressed C5aR at similar levels (Figure S7**C**). The two methods of functional inhibition of C5aR had little effect on IL1β secretion, indicating that the signal through C5aR plays no major role in this cell system (Figure 5**C**). Next, AS-treated cells were analyzed for surface binding of C3b fragments and MAC. Exposure to AS resulted in the higher binding of C3b fragments and MAC on PIGTKO cells compared with that on PIGAKO cells (Figures 5**D** and S8**A**, **B**). The level of MAC was several times higher on PIGTKO cells than on PIGAKO cells, suggesting that complement activation was enhanced, leading to the enhanced formation of MAC on PIGTKO cells. To confirm the role of MAC in IL1β secretion, PIGTKO cells were treated with acidified C6- and C7-depleted sera, in which C5a generation is intact whereas MAC formation is impaired. IL1β secretion was greatly reduced by C6 or C7 depletion and was restored by the replenishment of C6 or C7 (Figure 5**E**). These results suggest that MAC but not C5a plays a critical role in the secretion of IL1β. It is also suggested that free GPI plays some role in complement activation, leading to the enhanced binding of C3b fragments and MAC formation.

To determine whether the structure of free GPI (presence or absence of Gal capping) affects complement activation and subsequent IL1β secretion, we knocked out SLC35A2 in PIGTKO THP-1 cells. PIGT-SLC35A2 double-KO THP-1 cells were strongly stained by T5 mAb as expected (Figure S6**C**). The binding of both C3b fragments and MAC increased approximately five times after SLC35A2 KO (Figure 5**F**). Concomitantly, the secretion of IL1β more than doubled (Figure 5**G**). These results indicate that the structure of free GPI influenced complement activation efficiency and subsequent IL1β secretion.

Finally, we asked whether only the alternative pathway is involved in binding of C3b fragments on PIGTKO and PIGAKO THP-1 cells, or the lectin and/or the classical pathway is also involved. For this, cells were stained with anti-C4d mAb after treatment with acidified serum because activation of either pathway would result in binding of C4b, which is in turn converted to C4d (31, 32). C4d fragments were bound on PIGTKO cells and the binding was inhibited by 100 mM mannose by approximately 50% but not by N-acetylglucosamine (Figure 5**H**, top and Figure S8**D**). Binding of C3b fragments on PIGTKO cells was also inhibited by mannose by approximately 60% but not by N-acetylglucosamine (Figure 5**H**, bottom). These results suggest that the lectin pathway was activated on PIGTKO THP-1 cells, accounting for at least 60% of C3b fragments. C4d fragments were bound on PIGAKO cells at lower levels (60-70% of PIGTKO cell levels), which were not inhibited by either N-acetylglucosamine or mannose. Mannose, but not N-acetylglucosamine, mildly inhibited binding of C3b fragments on PIGAKO cells (Figure 5**H**). It is unclear at the moment whether the classical pathway was involved in residual C4d binding on PIGTKO cells in the presence of 100 mM mannose or in C4d binding on PIGAKO cells.

Discussion

We studied patients with PNH caused by *PIGT* mutations. Because PNH caused by *PIGT* mutations is characterized by autoinflammatory symptoms, we propose that they represent a new disease entity, PIGT-PNH. Patients with PIGT-PNH had a germline heterozygous mutation in the *PIGT* gene in combination with somatic deletion of the normal *PIGT* gene. Germline *PIGT* mutations were reported in patients with inherited GPI deficiency (IGD) (Table S2), which is characterized by developmental delay, seizures, hypotonia, and typical facial dysmorphism (11, 33-39). Inflammatory symptoms and intravascular hemolysis were not reported in IGD patients with *PIGT* mutations. They had either partial loss-of-function homozygous mutations, or combinations of a partial loss-of-function mutation and a null or nearly null mutation. Therefore, cells from the patients with IGD have only partially reduced PIGT activities and express only partially reduced levels of CD59 and DAF/CD55, and may have free GPI only to a small extent. In contrast, both germline and somatic mutants in PIGT-PNH were functionally null or nearly null (Table 1). Therefore, the affected cells from PIGT-PNH patients lost CD59 and DAF/CD55 severely or completely and had high levels of free GPI. Interestingly, the same mutation c.250G>T (p.E84X) was found in J1 and two Japanese patients with IGD (11, 37) who were not related to each other. PIGT-PNH patient J1 and mothers of two IGD patients from families 2 and 7 had the same heterozygous non-sense *PIGT* mutation (Table 1 and Table S2). These mothers were healthy and no inflammatory symptoms were reported for them (11, 37), suggesting that autoinflammation of J1 was not caused by haploinsufficiency of PIGT but was initiated after the somatic loss of the other *PIGT* copy occurred. Inheritance of the germline *PIGT* mutations in PIGT-PNH patients is not formally proven because DNA samples were not available from their families. A reported allele frequency of the germline variant *PIGT* of J1 and two Japanese families of IGD, c.250G>T (p.E84X), is 0.0002316 in the East Asian population, suggesting that 55,000 Japanese may have this variant (40). It is, therefore, highly likely that J1 inherited the *PIGT* variant.

The expansion of *PIGA*-defective clones in PNH is caused by selective survival under autoimmune bone marrow failure in most cases (41-43). This mechanism was first formulated by Rotoli and Luzzatto in 1989 (41). In few cases, clonal PNH cells acquired benign tumor characteristics by additional somatic mutations (44-46). In contrast, none of the patients with PIGT-PNH had documented bone marrow failure (Figure S1**A**) (7, 8). In addition, the myeloid CDR is lost in *PIGT*-defective clones in PIGT-PNH, similar to the case in clonal cells in myeloproliferative 20q− syndromes. The causal relationship between the myeloid CDR loss in PIGT-PNH and clonal expansion needs to be proven, particularly because boosted lineages under L3MBTL1 and SGK2 loss differ between in vitro study (13) and PIGT-PNH patients, and because platelet and leukocyte counts were not much changed in PIGT-PNH patients (Figure S1**A**). Complement dysregulation, which is present in PIGT-PNH but not in myeloproliferative 20q− syndromes, might modulate blood cell profiles. Nevertheless, this unique deletion occurs in PIGT-PNH but not in PIGA-PNH. Taking these findings together, it is likely that the mechanism of clonal expansion for PIGT-PNH is distinct from that for PIGA-PNH cells (see models in Figure S3**B**).

Whereas PIGT-PNH shares intravascular hemolysis and thrombosis with PNH, PIGT-PNH is characterized by autoinflammatory symptoms including recurrent urticaria, arthralgia and aseptic meningitis. PIGT-PNH first manifested with autoinflammatory symptoms alone and symptoms of PNH became apparent many years later (Table 1). It is possible that different clinical symptoms appear depending on the size of the *PIGT*-defective clone. When the clone size is small, autoinflammation but not PNH may occur and, when the clone size becomes sufficiently large, PNH may become apparent. The idea that the *PIGT*-defective clone is small when only autoinflammation is seen was supported by analyzing J1 DNA obtained before the start of recurrent hemolysis, only approximately 3% of total leukocytes being *PIGT*-defective (Figure 3**G**). Inflammatory symptoms, recurrent urticaria, arthralgia, fever, and especially meningitis seen in PIGT-PNH are shared by children with cryopyrinopathies or cryopyrin-associated periodic syndrome

(reviewed by Neven et al (47)). Cryopyrinopathies are caused by gain-of-function mutation in *NLRP3* that leads to easy activation of NLRP3 inflammasomes in monocytes and autoinflammatory symptoms (47), further suggesting that inflammasomes are activated in monocytes from PIGT-PNH patients. It was reported that autoinflammation occurs in patients having mosaicism with *NLRP3*-mutant cells even when the mutant clone size is small (frequency of mutant allele in whole blood cells being 4.3% to 6.5%) (48). This is relevant to the symptoms/clone size relationship in PIGT-PNH as discussed above.

C5 activation must be involved in the autoinflammatory symptoms in PIGT-PNH because they were suppressed by eculizumab. It is important to consider GPI-AP deficiency for patients with recurrent autoinflammatory symptoms such as aseptic meningitis even when PNH symptoms are absent because eculizumab may be effective for such cases. Because DAF and CD59 are missing on *PIGT*-defective monocytes, C5a and MAC might be generated once complement activation has been initiated. It was reported that subarachnoidal application of C5a in rabbits and rats induced acute experimental meningitis (49). Various types of myeloid cells are present in the central nervous system (reviewed in (50)). If C5 activation occurs on some of those cells lacking complement regulatory function and C5a is generated, aseptic meningitis might ensue.

The involvement of complement in inflammasome activation has been shown in various blood cell systems (51-54). Indeed, in the THP-1 cell model system, IL1β secretion was induced by complement in both PIGTKO and PIGAKO cells and more strongly in PIGTKO cells, mainly through MAC formation (Figure 5**A**, **B** and **E**). PIGT-PNH mononuclear cells were activated by conventional stimulators of inflammasomes similar to or even stronger than healthy control cells. Because blood mononuclear cells were easily lysed by acidified serum, the effect of complement on inflammasome activation in mononuclear cells could not be addressed. Taking the obtained findings together with the results for THP-1 cells, we speculate that *PIGT*-deficient

monocytes show an enhanced inflammasome response when complement is activated. How free GPI is involved in inflammasome and complement activation needs to be further clarified to fully understand the mechanistic basis of PIGT-PNH.

PIGU is an essential component of GPI transamidase, forming a protein complex with PIGT, PIGS, PIGK, and GPAA1 (Figure 1**A**) (55). PIGU-defective cells do not express GPI-APs on their surface (55). The *PIGU* gene is localized at approximately 7.4 Mb centromeric to the myeloid CDR (Figure 2**A** and 2**B**), and regions of somatic deletions of 18 and 12 Mb in GPI-AP-defective cells from J1 and G2, respectively, included the entire *PIGU* gene as well as myeloid CDR and *PIGT* gene. The levels of PIGU protein in these cells would be around half of the normal levels. It appears unlikely that the 50% reduction in PIGU has a significant impact on these cells. The levels of PIGT protein in the same cells would be zero or very low because mutations in the remaining *PIGT* gene are a nonsense mutation (E84X) in J1 and a frameshift mutation (frameshift after G254) in G2. For any remaining PIGT protein, half of the normal amounts of PIGU protein would be excessive for making the GPI transamidase complex. However, it is conceivable that, if a similar somatic deletion including *PIGU* and myeloid CDR occurs in a hematopoietic stem cell of an individual who bears a germline *PIGU* loss-of-function mutation, PNH with autoinflammation caused by *PIGU* mutation might occur.

Eculizumab was used for patients with PIGT-PNH. There are similarity and difference between PIGT-PNH and PNH against treatments with eculizumab. Similar to PNH, eculizumab was effective in preventing intravascular hemolysis in PIGT-PNH. Also similar to PNH, eculizumab caused appearance of direct Coombs positive erythrocytes in patient G1, suggesting an induction of extravascular hemolysis (7). Patients G2 had residual hemolysis after start of eculizumab therapy, also suggesting extravascular hemolysis (Table 1). PIGTKO THP-1 cells accumulated higher levels of C3b fragments upon complement activation (Figure 5**D**) and the

affected erythrocytes from PIGT-PNH patients express free GPI (Figure 3**D**). Whether the free-GPI-bearing PNH erythrocytes from PIGT-PNH patients accumulate more C3b fragments than PNH erythrocytes from PIGA-PNH patients and hence are more prone to extravascular hemolysis is yet to be clarified.

A difference is that percent PIGT-PNH cells increased not only in erythrocytes but also in granulocytes after treatment with eculizumab (Figure 1**B**). It is well known that percent PNH erythrocytes increase after eculizumab treatment because intravascular destruction of PNH erythrocytes is prevented by eculizumab (4). However, a sharp increase in percent PNH granulocytes seen in G1, G3 and J1, has not been reported in PIGA-PNH (4). A possible explanation for the difference is that PIGT-PNH granulocytes might have been destroyed in the blood by complement-dependent mechanisms. MAC formation was much higher on PIGTKO THP-1 cells than on PIGAKO cells (Figure 5**D**). If levels of MAC formation on PIGT-defective granulocytes are similarly high, MAC-mediated cell lysis might occur and eculizumab might prevent it, leading to an increase of percent PNH granulocytes. Another possibility is that the commencement of eculizumab treatment was only coincident with the active phase of clonal expansion. Because hemolysis becomes apparent only when clone size has increased, it is still possible that use of eculizumab is not causally related to increase of PNH granulocytes but that eculizumab treatment was done during active clonal expansion.

Eculizumab was effective in preventing recurrent autoinflammatory symptoms of PIGT-PNH. After start of eculizumab therapy, aseptic meningitis has not occurred in patients G3 and J1, and other symptoms such as urticaria and arthralgia were also prevented (Figure 1**D**) (8). These autoinflammatory symptoms, therefore, are dependent upon C5 activation. Results with PIGTKO THP-1 cells indicated that IL1β secretion after complement activation was mediated by MAC rather than C5a (Figure 5**C**, **E**). Patient J1 had elevated levels of IL18 and serum amyloid A (Table 2).

After start of eculizumab, serum amyloid A level turned normal whereas IL18 levels remained 4- to 5-times of upper limit of normal. IL18 secretion in PIGT-PNH, therefore, is not dependent upon terminal complement activation. C3 activation on the surface of PIGT-defective cells was higher than that on PIGA-defective cells as suggested by experimental results with PIGTKO and PIGAKO THP-1 cells (Figure 5**D**, **E**). It appeared that the activation of the lectin pathway was enhanced leading to elevated levels of C3b fragment binding and MAC formation (Figure 5**D**, **H**). The C4d binding on PIGTKO cells was significantly inhibited by mannose, suggesting that recognition of mannose residues in free GPIs by complement lectins might be involved in the lectin pathway activation. It seems likely that enhanced C3 activation is involved in the elevation of serum IL18 levels because C3 activation continues on PIGT-defective cell-surface during eculizumab therapy. Causal relationship between free GPIs and C3 activation, and molecular mechanisms involved need to be clarified to know whether earlier steps in complement activation are involved in pathogenesis of PIGT-PNH.

Materials and Methods

Blood samples and flow cytometry

Peripheral blood samples were obtained from patients J1 (8), G1 (7), G2 and G3 with PIGT-PNH, and six patients with PNH after informed consent. Peripheral blood leukocytes (Figure S1**B**), erythrocytes and reticulocytes were stained for GPI-APs by fluorescence-labeled non-lytic aerolysin (FLAER) (Cederlane), anti-CD14 (clone MOP9, BD Biosciences), -CD16 (clone 3G8, BioLegend), -CD24 (clone ML5, BioLegend), -CD48 (BJ40, BioLegend), -CD59 (clone 5H8) (56) or -CD66b (clone 80H3, Beckman Coulter Immunotech). T5-4E10 mAb (T5 mAb) against free GPI of *Toxoplasma gondii* was a gift from Dr. J. F. Dubremetz (18). T5 mAb is now available from BEI Resources, NIAID, NIH (Bethesda, MD). T5 mAb recognizes mammalian free GPI bearing N-acetylgalactosamine (GalNAc) side-chain linked to the first mannose (Figure 3**A**)(19). T5 mAb does not bind to free GPI when galactose (Gal) is attached to GalNAc. Therefore, reactivity of T5 mAb to free GPI is affected by an expression level of Gal transferase that attaches Gal to the GalNAc. Other antibodies used were PE-anti-CD55/DAF (clone IA10, BD), PE-anti-CD88/C5aR (BioLegend) and anti-TfR (clone H68.4, Thermo Fisher). Cells were analyzed by a flow cytometer (MACSQuant Analyzer VYB or FACSCalibur) and FlowJo software.

DNA and RNA analyses

Granulocytes with PNH phenotype were separated from normal granulocytes by cell sorting after staining by FLAER. DNA was analyzed for mutations in genes involved in GPI-AP biosynthesis by target exome sequencing, followed by confirmation by Sanger sequencing (7). DNA was also analyzed by array comparative genomic hybridization for deletion (7). Methylation status of CpG was determined by bisulfite sequencing and a SNuPE assay (13). Total RNA was extracted with the RNeasy Mini Kit (Qiagen) including DNase digestion and DNA cleanup, and reverse transcription was performed with the SuperScript VILO cDNA Synthesis Kit (Invitrogen). Levels of *L3MBTL1*, *SGK2*, *IFT52*, *MYBL2, ABL* and *GAPDH*

mRNAs were analyzed by quantitative real-time PCR (Table S1).

Cell lines

PIGT-defective CHO cells and *PIGL*-defective CHO cells were reported previously (11, 57). CRISPR/Cas 9 system was used to generate *PIGT* and *PIGA* knockout (KO) human monocytic THP-1 cells (ATCC) (Table S1 for guide RNA sequences). KO cells were FACS sorted for GPI-AP negative cells. Each knockout cell was rescued by transfection of a corresponding cDNA. *SLC35A2* gene was knocked out in PIGTKO THP-1 cells by CRISPR/Cas9 system.

Inflammasome activation and IL1β measurements

Toll-like receptor 2 (TLR2) ligands, Pam_3CSK4 and *Staphylococcus aureus* LTA, are from InvivoGen (28, 58). ATP and MSU for activating inflammasomes are from Enzo Life Sciences and InvivoGen (28, 59). Peripheral blood mononuclear cells were stimulated by Pam_3CSK4 or LTA for 4 hr at 37℃ and after washing by ATP or MSU for 4 hr at 37℃. IL1β ELISA kit (BioLegend) was used to measure IL1β secreted into the supernatants. Polyclonal rabbit anti-IL1β antibody for western blotting was from Cell Signaling Technology. PIGAKO, PIGTKO and wild-type THP-1 cells were differentiated into adherent macrophages in complete RPMI 1640 medium containing 100 ng/ml phorbol 12-myristate 13-acetate (PMA; InvivoGen) for 3 hr, and then with fresh complete medium for overnight (60). For stimulation, medium was replaced with serum free medium with Pam_3CSK_4 (200 ng/ml), followed 4hr-later by ATP stimulation for 4 hr (5 mM).

Stimulation of THP-1-derived macrophages with complement

As a source of complement, whole blood was collected from healthy donors after informed consent, and serum separated, aliquoted and stored at -80°C prior to use. Inactivation of complement was carried out by heating serum at 56°C for 30 min. To prepare acidified serum (AS) that allows activation of the alternative pathway on the cell surface, 21 volumes of serum was mixed

with 1 volume of 0.4 M HCl to have pH of approximately 6.7. C6- and C7-depleted sera and purified C6 and C7 proteins were purchased from Complement Technology. Differentiated cells were stimulated with acidified normal serum, or acidified C6-depleted and C7-depleted sera, and those reconstituted with C6 and C7, respectively, at 37°C for 5hr and secreted IL1β was measured by ELISA. C5 was inhibited by addition of 35 μg/ml anti-C5 mAb (eculizumab, Alexion Pharmaceuticals).

For ex vivo blockade of human C5aR, anti-human C5aR or nonpeptide C5aR antagonist W-54011 (5 μM, Merck Millipore)(30) was used. Complement C3 and C4 fragments and MAC deposited on the cells were measured by flow cytometry. THP-1 cells were suspended in 20 μl FACS buffer (PBS, 1% BSA, 0.05% sodium azide) with 1:20 human TruStain FcX™ (Fc receptor blocking solution) at room temperature for 10 min. Cells were stained with anti-C3/C3b/iC3b/C3d mAb (clone 1H8, BioLegend), anti-C4d mAb (clone 12D11, Hycult Biotech) or rabbit anti-human SC5b-9 (MAC) polyclonal antibodies (Complement Technology) in FACS buffer. After washing twice, cells were incubated with the PE-conjugated goat anti-mouse IgG (BioLegend) or Alexa Fluor488-conjugated goat anti-rabbit IgG (Thermo Fisher) secondary antibody. The anti-human SC5b-9 polyclonal antibodies positively stained PMA-differentiated THP-1 cells without incubation in AS. The same antibodies did not stain similarly differentiated PIGTKO and PIGAKO THP-1 cells, suggesting that the antibody product contained antibodies reacted with some GPI-AP expressed on THP-1-derived macrophages (Figure S8**B**, **C**). Because of this reactivity to non-MAC antigen(s), the anti-SC5b-9 antibodies were used for PIGTKO and PIGAKO cells but not for WT cells in experiments shown in Figure 5**D** and **F**. To inhibit the lectin pathway, serum was mixed with mannose or N-acetylglucosamine (final concentration of 100 mM) before acidification (61).

Statistical analyses

All experiments with THP-1 cells were performed at least three times. All values were expressed as the mean ± SD of individual samples. For

two-group comparisons between PIGTKO and PIGAKO cells, two-tailed student's *t*-test was used. *P* values less than 0.05 were considered statistically significant.

Study approval

This study was approved by institutional review boards of Osaka University (approval number 681), University of Ulm (approval numbers 279/09 and 188/16) and University of Berlin (approval number EA2/077/12).

Data Sharing Statement

All data supporting the findings are available from the corresponding authors.

Author contributions

BH, YM, NI, HS, PMK, and TK designed research. YM, MO, AK, TH, Shogo M, TE, MJ, RF, and AH performed research. BH, MK, MA, Sho M, YU, and NK acquired the data. BH, YM, MO, MK, JN, YK, NK, HS, and PMK analyzed data. BH, YM, MO, HS, PMK, and TK wrote the paper. Three authors sharing the first author position are in alphabetical order.

Acknowledgements

We thank Drs. Morihisa Fujita (Jiangnan University), Tatsutoshi Nakahata (Kyoto University), Hidenori Ohnishi (Gifu University), Tatsuya Saitoh (Tokushima University) and Yusuke Maeda (Osaka University) for discussion, Dr. Jean-Francois Dubremetz (Montpellier University) for T5-4E10 mAb, Dr. Lucio Luzzatto (Muhimbili University) for critical reading and editing advice on this manuscript, and Keiko Kinoshita, Kana Miyanagi, Saori Umeshita and Miguel Rodriguez de los Santos for technical help and Dr. med. Lisa A. Gerdes (Munich University) for collaboration regarding patients G3 as well as the patients for providing blood samples and pictures. We thank Edanz (www.edanzediting.co.jp) for editing the English text of a draft of this manuscript. This work was supported by JSPS and MEXT KAKENHI grants (JP16H04753 and JP17H06422) to TK and a grant from the Japan Society of Complement Research to YM.

References

1. Parker C, Omine M, Richards S, Nishimura J, Bessler M, Ware R, Hillmen P, Luzzatto L, Young N, Kinoshita T, et al. Diagnosis and management of paroxysmal nocturnal hemoglobinuria. *Blood.* 2005;106(12):3699-3709.
2. Hill A, DeZern AE, Kinoshita T, and Brodsky RA. Paroxysmal nocturnal haemoglobinuria. *Nat Rev Dis Primers.* 2017;3:17028.
3. Takeda J, Miyata T, Kawagoe K, Iida Y, Endo Y, Fujita T, Takahashi M, Kitani T, and Kinoshita T. Deficiency of the GPI anchor caused by a somatic mutation of the PIG-A gene in paroxysmal nocturnal hemoglobinuria. *Cell.* 1993;73(4):703-711.
4. Hillmen P, Young NS, Schubert J, Brodsky RA, Socie G, Muus P, Roth A, Szer J, Elebute MO, Nakamura R, et al. The complement inhibitor eculizumab in paroxysmal nocturnal hemoglobinuria. *N Engl J Med.* 2006;355(12):1233-1243.
5. Hillmen P, Muus P, Roth A, Elebute MO, Risitano AM, Schrezenmeier H, Szer J, Browne P, Maciejewski JP, Schubert J, et al. Long-term safety and efficacy of sustained eculizumab treatment in patients with paroxysmal nocturnal haemoglobinuria. *Br J Haematol.* 2013;162(1):62-73.
6. Kinoshita T. Biosynthesis and deficiencies of glycosylphosphatidylinositol. *Proc Jpn Acad Ser B Phys Biol Sci.* 2014;90(4):130-143.
7. Krawitz PM, Hochsmann B, Murakami Y, Teubner B, Kruger U, Klopocki E, Neitzel H, Hoellein A, Schneider C, Parkhomchuk D, et al. A case of paroxysmal nocturnal hemoglobinuria caused by a germline mutation and a somatic mutation in PIGT. *Blood.* 2013;122(7):1312-1315.
8. Kawamoto M, Murakami Y, Kinoshita T, and Kohara N. Recurrent aseptic meningitis with PIGT mutations: a novel pathogenesis of recurrent meningitis successfully treated by eculizumab. *BMJ Case Rep.* 2018;2018(doi: 10.1136/bcr-2018-225910).

9. Ohishi K, Inoue N, and Kinoshita T. PIG-S and PIG-T, essential for GPI anchor attachment to proteins, form a complex with GAA1 and GPI8. *EMBO J.* 2001;20(15):4088-4098.
10. Wang Y, Hirata T, Maeda Y, Murakami Y, Fujita M, and Kinoshita T. Free, unlinked glycosylphosphatidylinositols on mammalian cell surfaces revisited. *J Biol Chem.* 2019;294(13):5038-5049.
11. Nakashima M, Kashii H, Murakami Y, Kato M, Tsurusaki Y, Miyake N, Kubota M, Kinoshita T, Saitsu H, and Matsumoto N. Novel compound heterozygous PIGT mutations caused multiple congenital anomalies-hypotonia-seizures syndrome 3. *Neurogenetics.* 2014;15(3):193-200.
12. Bench AJ, Nacheva EP, Hood TL, Holden JL, French L, Swanton S, Champion KM, Li J, Whittaker P, Stavrides G, et al. Chromosome 20 deletions in myeloid malignancies: reduction of the common deleted region, generation of a PAC/BAC contig and identification of candidate genes. UK Cancer Cytogenetics Group (UKCCG). *Oncogene.* 2000;19(34):3902-3913.
13. Aziz A, Baxter EJ, Edwards C, Cheong CY, Ito M, Bench A, Kelley R, Silber Y, Beer PA, Chng K, et al. Cooperativity of imprinted genes inactivated by acquired chromosome 20q deletions. *J Clin Invest.* 2013;123(5):2169-2182.
14. Araten DJ, Swirsky D, Karadimitris A, Notaro R, Nafa K, Bessler M, Thaler HT, Castro-Malaspina H, Childs BH, Boulad F, et al. Cytogenetic and morphological abnormalities in paroxysmal nocturnal haemoglobinuria. *Br J Haematol.* 2001;115(2):360-368.
15. Sloand EM, Fuhrer M, Keyvanfar K, Mainwaring L, Maciejewski J, Wang Y, Johnson S, Barrett AJ, and Young NS. Cytogenetic abnormalities in paroxysmal nocturnal haemoglobinuria usually occur in haematopoietic cells that are glycosylphosphatidylinositol-anchored protein (GPI-AP) positive. *Br J Haematol.* 2003;123(1):173-176.
16. Li J, Bench AJ, Vassiliou GS, Fourouclas N, Ferguson-Smith AC, and Green AR. Imprinting of the human L3MBTL gene, a polycomb family member located in a region of chromosome 20 deleted in human

myeloid malignancies. *Proc Natl Acad Sci USA.* 2004;101(19):7341-7346.

17. Miyata T, Takeda J, Iida Y, Yamada N, Inoue N, Takahashi M, Maeda K, Kitani T, and Kinoshita T. Cloning of PIG-A, a component in the early step of GPI-anchor biosynthesis. *Science.* 1993;259(5099):1318-1320.
18. Tomavo S, Couvreur G, Leriche MA, Sadak A, Achbarou A, Fortier B, and Dubremetz JF. Immunolocalization and characterization of the low molecular weight antigen (4-5 kDa) of Toxoplasma gondii that elicits an early IgM response upon primary infection. *Parasitology.* 1994;108(Pt 2):139-145.
19. Hirata T, Mishra SK, Nakamura S, Saito K, Motooka D, Takada Y, Kanzawa N, Murakami Y, Maeda Y, Fujita M, et al. Identification of a Golgi GPI-N-acetylgalactosamine transferase with tandem transmembrane regions in the catalytic domain. *Nat Commun.* 2018;9(1):405.
20. Murakami Y, Kanzawa N, Saito K, Krawitz PM, Mundlos S, Robinson PN, Karadimitris A, Maeda Y, and Kinoshita T. Mechanism for release of alkaline phosphatase caused by glycosylphosphatidylinositol deficiency in patients with hyperphosphatasia mental retardation syndrome. *J Biol Chem.* 2012;287(9):6318-6325.
21. Buckley JT. In: Alouf JE, and Freer JH eds. *The Comprehensive Sourcebook of Bacterial Protein Toxins*. London: Academic Press; 1999:362-372.
22. Kooyman DL, Byrne GW, McClellan S, Nielsen D, Tone M, Waldmann H, Coffman TM, McCurry KR, Platt JL, and Logan JS. In vivo transfer of GPI-linked complement restriction factors from erythrocytes to the endothelium. *Science.* 1995;269(5220):89-92.
23. Dunn DE, Yu J, Nagarajan S, Devetten M, Weichold FF, Medof ME, and Young NS. A knock-out model of paroxysmal nocturnal hemoglobinuria: Pig-a- hematopoiesis is reconstituted following intercellular transfer of GPI-anchored proteins. *Proc Natl Acad Sci USA.* 1996;93(15):7938-7943.

24. Brodsky RA, Mukhina GL, Li S, Nelson KL, Chiurazzi PL, Buckley JT, and Borowitz MJ. Improved detection and characterization of paroxysmal nocturnal hemoglobinuria using fluorescent aerolysin. *Am J Clin Pathol.* 2000;114(3):459-466.
25. Diep DB, Nelson KL, Raja SM, Pleshak EN, and Buckley JT. Glycosylphosphatidylinositol anchors of membrane glycoproteins are binding determinants for the channel-forming toxin aerolysin. *J Biol Chem.* 1998;273(4):2355-2360.
26. Abrami L, Velluz MC, Hong Y, Ohishi K, Mehlert A, Ferguson M, Kinoshita T, and Gisou van der Goot F. The glycan core of GPI-anchored proteins modulates aerolysin binding but is not sufficient: the polypeptide moiety is required for the toxin- receptor interaction. *FEBS Lett.* 2002;512(1-3):249-254.
27. Hong Y, Ohishi K, Inoue N, Kang JY, Shime H, Horiguchi Y, van der Goot FG, Sugimoto N, and Kinoshita T. Requirement of *N*-glycan on GPI-anchored proteins for efficient binding of aerolysin but not *Clostridium septicum* a-toxin. *EMBO J.* 2002;21(19):5047-5056.
28. Parzych K, Zetterqvist AV, Wright WR, Kirkby NS, Mitchell JA, and Paul-Clark MJ. Differential role of pannexin-1/ATP/P2X7 axis in IL-1beta release by human monocytes. *FASEB J.* 2017;31(6):2439-2445.
29. Ricklin D, Hajishengallis G, Yang K, and Lambris JD. Complement: a key system for immune surveillance and homeostasis. *Nat Immunol.* 2010;11(9):785-797.
30. Sumichika H, Sakata K, Sato N, Takeshita S, Ishibuchi S, Nakamura M, Kamahori T, Ehara S, Itoh K, Ohtsuka T, et al. Identification of a potent and orally active non-peptide C5a receptor antagonist. *J Biol Chem.* 2002;277(51):49403-49407.
31. Fujita T, Endo Y, and Nonaka M. Primitive complement system--recognition and activation. *Mol Immunol.* 2004;41(2-3):103-111.
32. Fujita T, Matsushita M, and Endo Y. The lectin-complement pathway--its role in innate immunity and evolution. *Immunol Rev.*

2004;198:185-202.

33. Kvarnung M, Nilsson D, Lindstrand A, Korenke GC, Chiang SC, Blennow E, Bergmann M, Stodberg T, Makitie O, Anderlid BM, et al. A novel intellectual disability syndrome caused by GPI anchor deficiency due to homozygous mutations in PIGT. *J Med Genet.* 2013;50(8):521-528.
34. Lam C, Golas GA, Davids M, Huizing M, Kane MS, Krasnewich DM, Malicdan MC, Adams DR, Markello TC, Zein WM, et al. Expanding the clinical and molecular characteristics of PIGT-CDG, a disorder of glycosylphosphatidylinositol anchors. *Mol Genet Metab.* 2015;115(2-3):128-140.
35. Skauli N, Wallace S, Chiang SC, Baroy T, Holmgren A, Stray-Pedersen A, Bryceson YT, Stromme P, Frengen E, and Misceo D. Novel PIGT variant in two brothers: Expansion of the multiple congenital anomalies-hypotonia seizures syndrome 3 phenotype. *Genes (Basel).* 2016;7(12):pii: E108.
36. Pagnamenta AT, Howard MF, Taylor JM, Miller V, Johnson DS, Tadros S, Mansour S, Temple IK, Firth R, Rosser E, et al. Analysis of exome data for 4293 trios suggests GPI-anchor biogenesis defects are a rare cause of developmental disorders. *Eur J Hum Genet.* 2017;25(6):669-679.
37. Kohashi K, Ishiyama A, Yuasa S, Tanaka T, Miya K, Adachi Y, Sato N, Saitsu H, Ohba C, Matsumoto N, et al. Epileptic apnea in a patient with inherited glycosylphosphatidylinositol anchor deficiency and PIGT mutations. *Brain Dev.* 2018;40(1):53-57.
38. Yang L, Peng J, Yin XM, Pang N, Chen C, Wu TH, Zou XM, and Yin F. Homozygous PIGT Mutation Lead to Multiple Congenital Anomalies-Hypotonia Seizures Syndrome 3. *Front Genet.* 2018;9(153.
39. Bayat A, Knaus A, Juul AW, Dukic D, Gardella E, Charzewska A, Clement E, Hjalgrim H, Hoffman-Zacharska D, Horn D, et al. PIGT-CDG, a disorder of the glycosylphosphatidylinositol anchor: description of 13 novel patients and expansion of the clinical characteristics. *Genet Med.* 2019;10.1038/s41436-019-0512-3(

40. Lek M, Karczewski KJ, Minikel EV, Samocha KE, Banks E, Fennell T, O'Donnell-Luria AH, Ware JS, Hill AJ, Cummings BB, et al. Analysis of protein-coding genetic variation in 60,706 humans. *Nature.* 2016;536(7616):285-291.
41. Rotoli B, and Luzzatto L. Paroxysmal nocturnal hemoglobinuria. *Semin Hematol.* 1989;26(3):201-207.
42. Young NS. The problem of clonality in aplastic anemia: Dr Dameshek's riddle, restated. *Blood.* 1992;79(6):1385-1392.
43. Luzzatto L, Bessler M, and Rotoli B. Somatic mutations in paroxysmal nocturnal hemoglobinuria: A blessing in disguise? *Cell.* 1997;88(1-4.
44. Inoue N, Izui-Sarumaru T, Murakami Y, Endo Y, Nishimura J, Kurokawa K, Kuwayama M, Shime H, Machii T, Kanakura Y, et al. Molecular basis of clonal expansion of hematopoiesis in 2 patients with paroxysmal nocturnal hemoglobinuria (PNH). *Blood.* 2006;108(13):4232-4236.
45. Shen W, Clemente MJ, Hosono N, Yoshida K, Przychodzen B, Yoshizato T, Shiraishi Y, Miyano S, Ogawa S, Maciejewski JP, et al. Deep sequencing reveals stepwise mutation acquisition in paroxysmal nocturnal hemoglobinuria. *J Clin Invest.* 2014;124(10):4529-4538.
46. Luzzatto L, and Risitano AM. Advances in understanding the pathogenesis of acquired aplastic anaemia. *Br J Haematol.* 2018;182(6):758-776.
47. Neven B, Prieur AM, and Quartier dit Maire P. Cryopyrinopathies: update on pathogenesis and treatment. *Nat Clin Pract Rheumatol.* 2008;4(9):481-489.
48. Saito M, Nishikomori R, Kambe N, Fujisawa A, Tanizaki H, Takeichi K, Imagawa T, Iehara T, Takada H, Matsubayashi T, et al. Disease-associated CIAS1 mutations induce monocyte death, revealing low-level mosaicism in mutation-negative cryopyrin-associated periodic syndrome patients. *Blood.* 2008;111(4):2132-2141.
49. Faustmann PM, Krause D, Dux R, and Dermietzel R. Morphological study in the early stages of complement C5a fragment-induced

experimental meningitis: activation of macrophages and astrocytes. *Acta Neuropathol.* 1995;89(3):239-247.

50. Herz J, Filiano AJ, Smith A, Yogev N, and Kipnis J. Myeloid Cells in the Central Nervous System. *Immunity.* 2017;46(6):943-956.
51. An LL, Mehta P, Xu L, Turman S, Reimer T, Naiman B, Connor J, Sanjuan M, Kolbeck R, and Fung M. Complement C5a potentiates uric acid crystal-induced IL-1beta production. *Eur J Immunol.* 2014;44(12):3669-3679.
52. Samstad EO, Niyonzima N, Nymo S, Aune MH, Ryan L, Bakke SS, Lappegard KT, Brekke OL, Lambris JD, Damas JK, et al. Cholesterol crystals induce complement-dependent inflammasome activation and cytokine release. *J Immunol.* 2014;192(6):2837-2845.
53. Laudisi F, Spreafico R, Evrard M, Hughes TR, Mandriani B, Kandasamy M, Morgan BP, Sivasankar B, and Mortellaro A. Cutting edge: the NLRP3 inflammasome links complement-mediated inflammation and IL-1beta release. *J Immunol.* 2013;191(3):1006-1010.
54. Arbore G, West EE, Spolski R, Robertson AA, Klos A, Rheinheimer C, Dutow P, Woodruff TM, Yu ZX, O'Neill LA, et al. T helper 1 immunity requires complement-driven NLRP3 inflammasome activity in CD4(+) T cells. *Science.* 2016;352(6292):aad1210.
55. Hong Y, Ohishi K, Kang JY, Tanaka S, Inoue N, Nishimura J, Maeda Y, and Kinoshita T. Human PIG-U and yeast Cdc91p are the fifth subunit of GPI transamidase that attaches GPI-anchors to proteins. *Mol Biol Cell.* 2003;14(5):1780-1789.
56. Sugita Y, Ito K, Shiozuka K, Suzuki H, Gushima H, Tomita M, and Masuho Y. Recombinant soluble CD59 inhibits reactive haemolysis with complement. *Immunology.* 1994;82(1):34-41.
57. Nakamura N, Inoue N, Watanabe R, Takahashi M, Takeda J, Stevens VL, and Kinoshita T. Expression cloning of PIG-L, a candidate N-acetylglucosaminyl-phosphatidylinositol deacetylase. *J Biol Chem.* 1997;272(25):15834-15840.
58. Morath S, Geyer A, and Hartung T. Structure-function relationship of

cytokine induction by lipoteichoic acid from Staphylococcus aureus. *J Exp Med.* 2001;193(3):393-397.

59. Martinon F, Petrilli V, Mayor A, Tardivel A, and Tschopp J. Gout-associated uric acid crystals activate the NALP3 inflammasome. *Nature.* 2006;440(7081):237-241.

60. Zhou R, Yazdi AS, Menu P, and Tschopp J. A role for mitochondria in NLRP3 inflammasome activation. *Nature.* 2011;469(7329):221-225.

61. Matsushita M, Endo Y, Taira S, Sato Y, Fujita T, Ichikawa N, Nakata M, and Mizuochi T. A novel human serum lectin with collagen- and fibrinogen-like domains that functions as an opsonin. *J Biol Chem.* 1996;271(5):2448-2454.

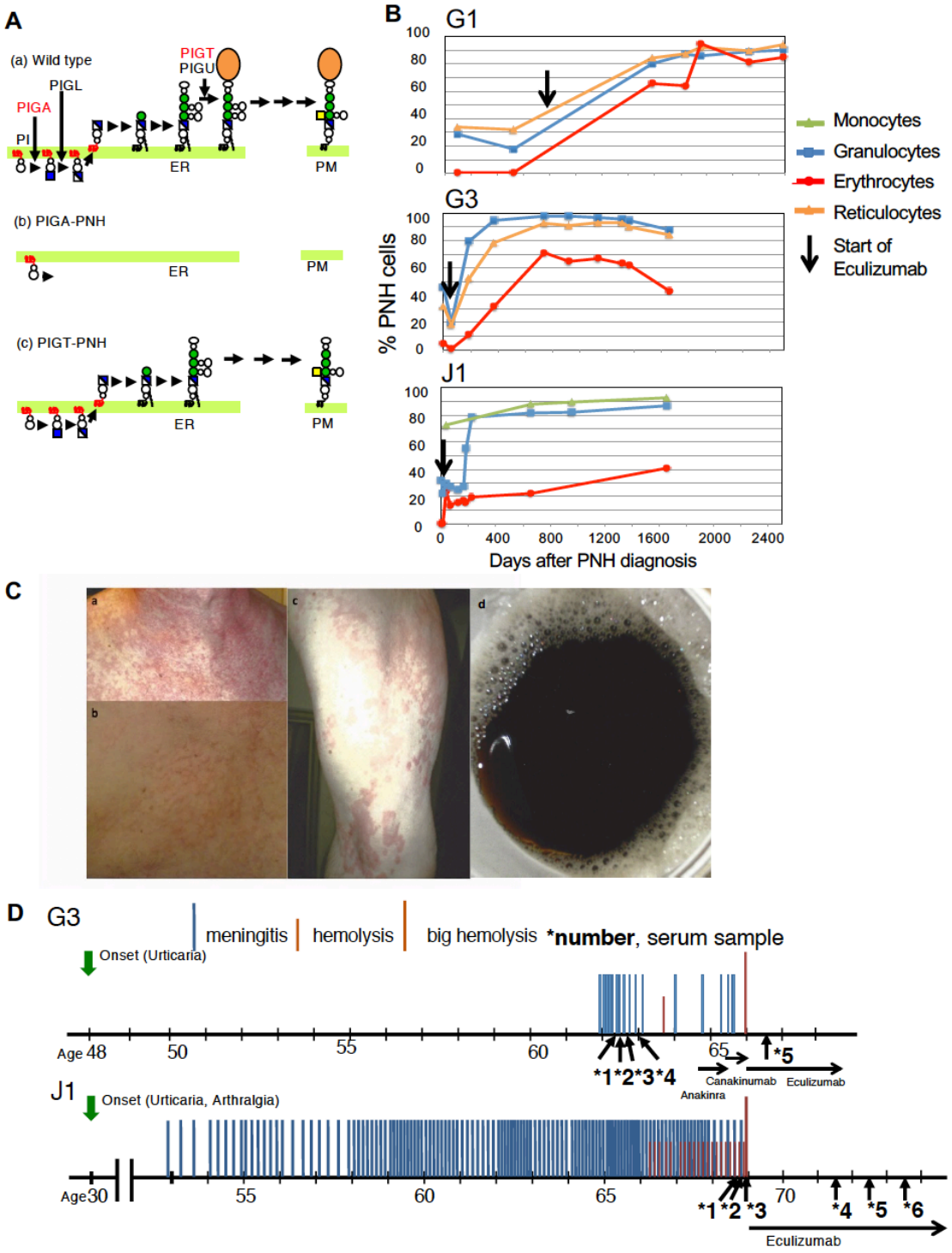

Figure 1. Clinical features of PIGT-PNH. A. Schematics of normal and defective biosynthesis of GPI-APs. (a) In normal cells, GPI is synthesized in the endoplasmic reticulum (ER) from phosphatidylinositol (PI) by sequential reactions and assembled GPI is attached to proteins (orange oval). PIGA acts in the first step whereas PIGT acts in attachment of GPI to proteins.

GPI-APs are transported to the plasma membrane (PM). (b) No GPI biosynthesis in PNH caused by *PIGA* defect. (c) Accumulation of free GPI in PNH cells caused by *PIGT* defect. Un-protein-linked GPI is transported to the PM. **B.** Time course of PNH clone sizes in patients G1, G3 and J1. Percentages of PNH cells in monocytes, granulocytes, erythrocytes and reticulocytes are plotted as a function of time in days. Arrows, start of eculizumab therapy. **C**. Examples of urticaria in G3 before the start of the anakinra treatment: (a) and (b), chest; (c), left upper leg. Brightness in (b) was adjusted to more clearly show raised skin in the affected area. (d) hemoglobinuria of patient G3. The pictures were kindly made available by the patient. **D**. Clinical courses of G3 in comparison to J1 (Figure 1 in Kawamoto M et al (8) was modified with additional data) including effective treatments. G3 (top) had meningitis 19 times since 62 to 65 years of age. Eculizumab therapy started at 66 years of age after a severe hemolysis. J1 (bottom) had meningitis 121 times since 53 to 69 years of age when eculizumab therapy started. Downward green arrows, onset of urticaria and/or arthralgia; Blue middle height bars, meningitis; Orange short bars, hemolysis; Orange long bars, severe hemolysis; horizontal arrows of various lengths, treatment periods of effective therapies (Anakinra and canakinumab were given with prednisolone); upward arrows with number and asterisk, serum samples taken for cytokine and other protein determination.

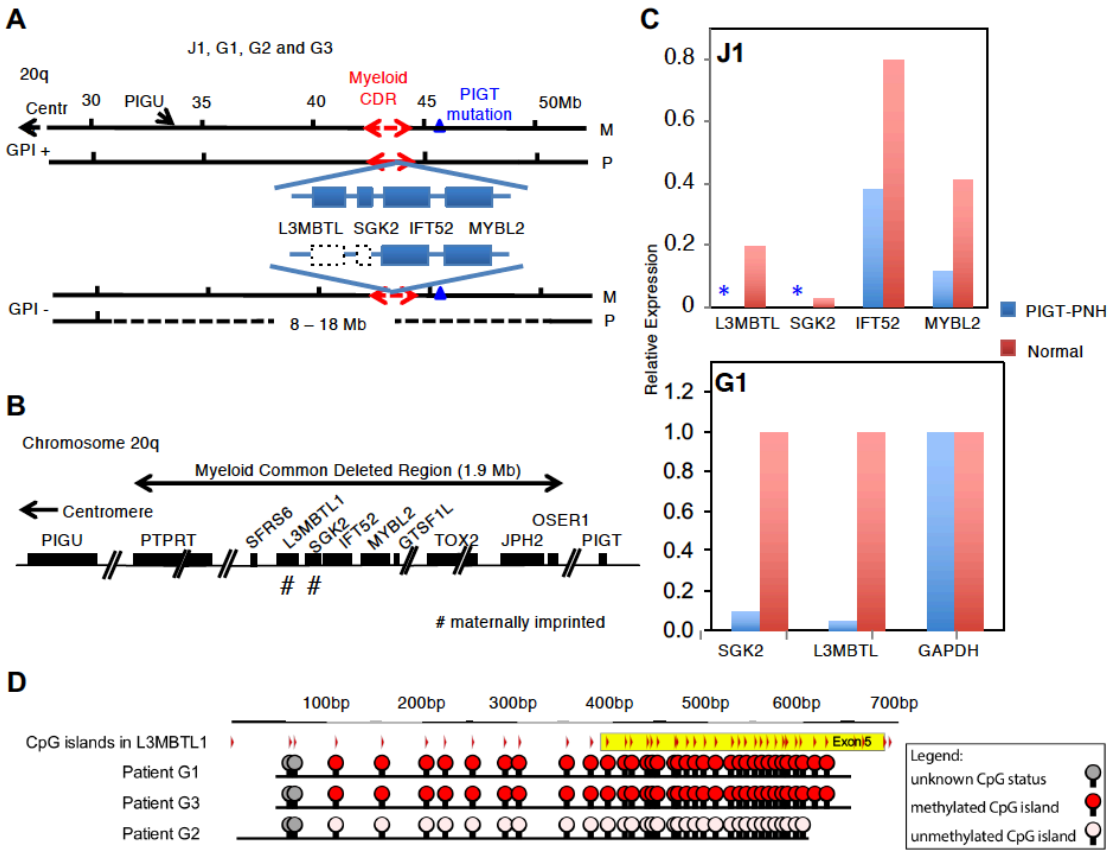

Figure 2. Genetic abnormalities in patients with PIGT-PNH. A. PIGT mutations in GPI-AP-positive (GPI +) and -defective (GPI -) cells from patients with PIGT-PNH. (Top) GPI + cells from patients J1, G1, G2 and G3 had a germline *PIGT* mutation (triangle) in the maternal (M) allele. Two maternally imprinted genes, *L3MBTL1* and *SGK2*, within myeloid Common Deleted Region (CDR) are expressed from the paternal (P) allele. Solid and broken red double arrows, P and M alleles of myeloid CDR, respectively. (Bottom) GPI - blood cells from PIGT-PNH patients had an 8 Mb to 18 Mb deletion spanning myeloid CDR and *PIGT* and/or *PIGU* in the P chromosome 20q leading to losses of expression of *L3MBTL1* and *SGK2* genes (dotted boxes). **B**. Myeloid Common Deleted Region. A 1.9-Mb region in chromosome 20q spanning *PTPRT* gene to *OSER1* gene is termed "myeloid common deleted region (CDR)". *PIGT* and *PIGU* genes are approximately 1.2 Mb telomeric and 7.4 Mb centromeric to the myeloid CDR, respectively. *L3MBTL1* and *SGK2* genes marked # are maternally imprinted. **C**. qRT-PCR

analysis of genes within myeloid CDR in GPI-AP-defective granulocytes from J1 and granulocytes from a healthy control (top) and whole blood cells from G1 and a healthy control (bottom). L3MBTL1 and SGK2, maternally imprinted genes; IFT52 and MYBL2, non-imprinted genes. Relative expression is determined taking means of ABL levels as 1 (J1) or of GAPDH as 1 (G1). Blue bars, cells from J1 and G1; orange bars, cells from healthy individuals; asterisks (*), below detection limits. Mean of duplicate (JI) and triplicate (G1) samples in one of the two independent experiments. Mean RQ max values for J1 samples were 0.15 (IFT52) and 0.17 (MYBL2), and for normal control samples were 0.034 (L3MBLT), 0.003 (SGK2), 0.078 (IFT52) and 0.002 (MYBL2). Mean RQ max values for G1 samples were 0.01 (SGK2), 0.004 (L3MBTL) and 0.01 (GAPDH), and for normal control samples were 0.08 (SGK2), 0.22 (L3MBTL) and 0.002 (GAPDH). **D**. Methylation status of the CpG islands in *L3MBTL1* in G1, G2 and G3. Red, methylated CpG islands; pink, unmethylated CpG islands; gray, unknown CpG islands. Bisulfite sequencing data are shown in Figure S3**A**.

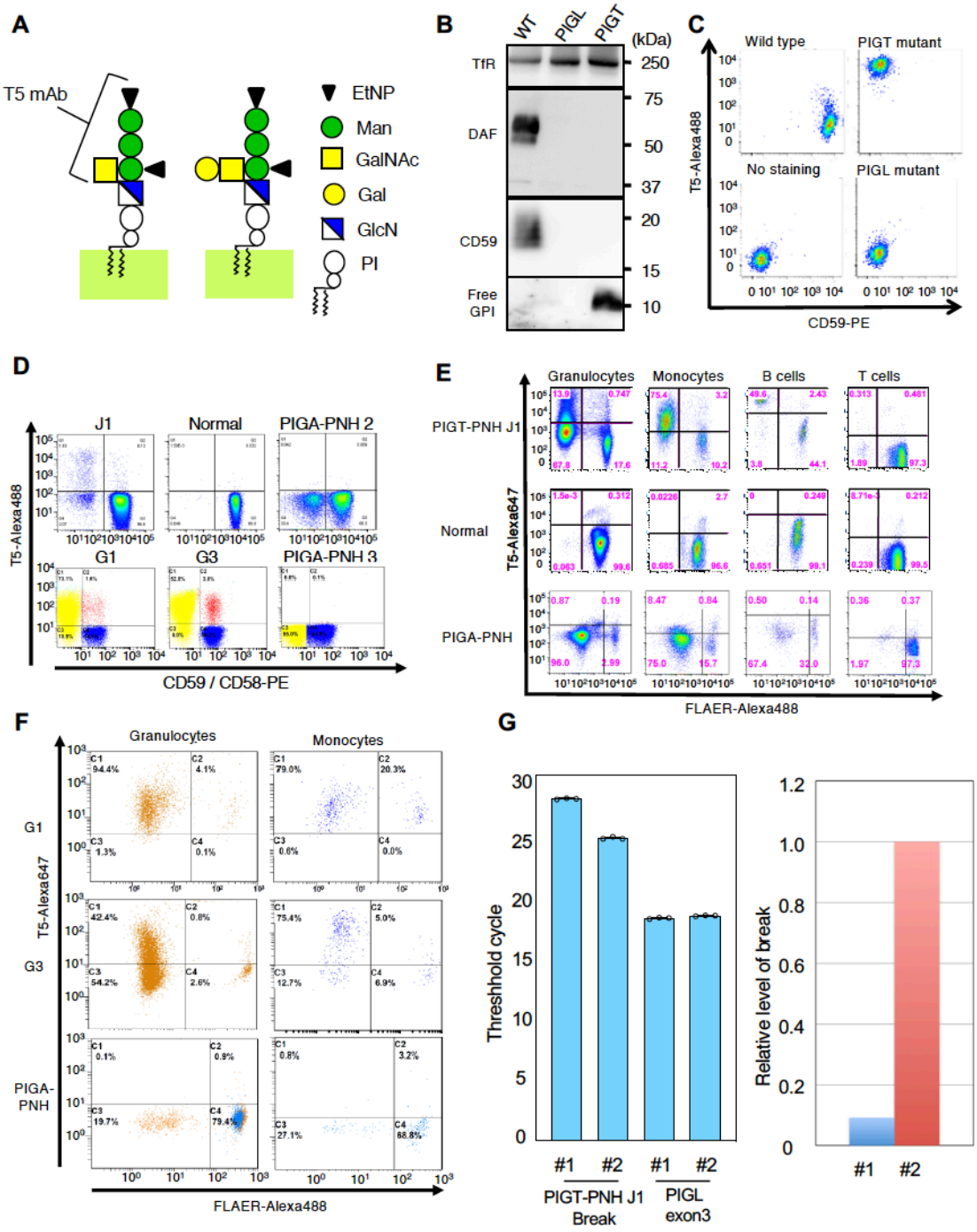

Figure 3. Biochemical abnormalities in PIGT-defective cells. A. Schematic representation of binding specificity of T5 mAb. T5 mAb recognizes mammalian free GPI bearing GalNAc-side chain linked to the first mannose (left). T5 mAb does not bind to free GPI when Gal is attached to GalNAc (right). Man, mannose; GlcN, glucosamine; EtNP, ethanolamine phosphate;

PI, phosphatidylinositol. **B**. Western blotting analysis of *PIGT*-defective and *PIGL*-defective CHO cells with T5 mAb for free GPI, anti-CD59 and anti-DAF mAbs, and anti-transferrin receptor (TfR) as loading controls. **C**. Flow cytometry of *PIGT*-defective and *PIGL*-defective CHO cells with T5 mAb and anti-CD59 mAb. **D**. Flow cytometry of erythrocytes from J1, G1, G3, a healthy individual and two patients with PIGA-PNH with T5 mAb and anti-CD59 (top panels) or anti-CD58 (bottom panels). **E**. Flow cytometry of blood cells from JI, a healthy individual and a patient with PIGA-PNH with T5 mAb and FLAER. **F**. Granulocytes and monocytes from G1 and G3, and a patient with PIGA-PNH, stained by T5 mAb and FLAER. **G**. Determination of the PNH clone size in J1 by qPCR analysis of the break causing 18 Mbp deletion. (Left) Threshold cycle in PCR for the break and exon 3 of PIGL as a reference. #1, DNA from whole blood leukocytes taken in a stage with autoinflammation only (four months before the onset of recurrent hemolysis); #2, DNA from granulocytes (29% of cells were GPI-AP-defective) taken one month after start of eculizumab therapy. (Right) Relative levels of the break in samples #1 and #2 by setting the level in #2 as 1. Data are shown in mean of triplicate samples in one experiment. Mean RQ max values for #1 and #2 samples were 0.092 and 1.11, respectively.

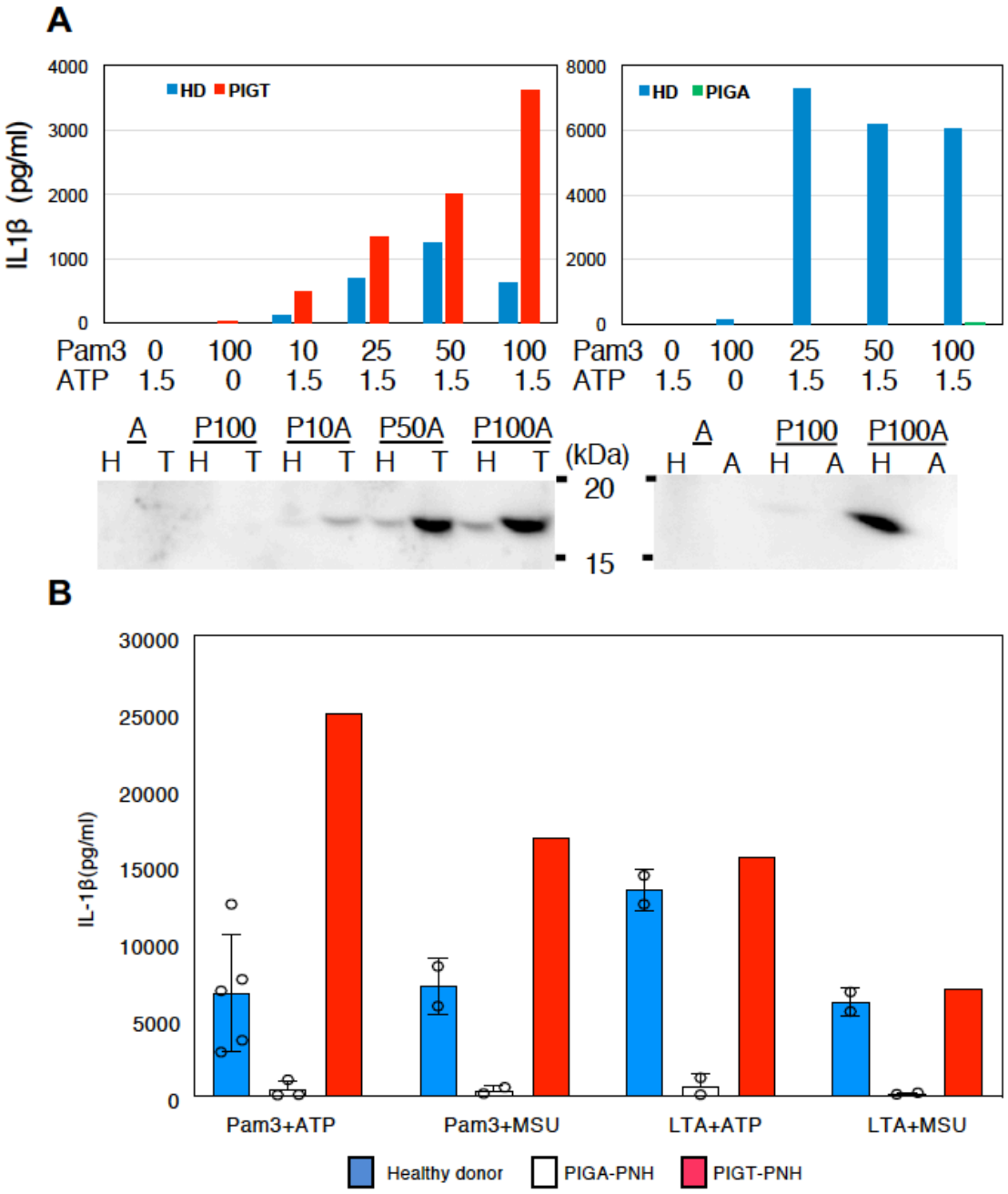

Figure 4. IL1β secretion from PIGT-PNH and PIGA-PNH cells. A. The peripheral blood mononuclear cells from JI, PIGA-PNH4 and a healthy individual were incubated with 10 to 100 ng/ml Pam_3CSK4 (Pam3) at 37℃ for 4 hr, and then were incubated with 1.5 mM ATP for 30 min. IL1β in the supernatants was measured by ELISA (top) and western blotting (bottom). (Left) J1 (red bars) and a healthy individual (blue bars). (Right) PIGA-PNH4 (green bars) and a healthy individual (blue bars). A, ATP only; P100, 100 ng/ml Pam_3CSK4 only; P10A, P50A and P100A, 10, 50 and 100 ng/ml

Pam_3CSK4, respectively and ATP; H, healthy donors; T, PIGT-PNH; A, PIGA-PNH. **B**. The peripheral blood mononuclear cells from J1, two or three patients with PIGA-PNH, and two or five healthy controls were stimulated with 200 ng/ml of Pam3 or 1 μg/ml of lipoteichoic acid (LTA) from *Staphylococcus aureus* for 4 hr at 37℃ and after washing were incubated with 3mM ATP or 200 μg/ml monosodium ureate (MSU) for 4 hr at 37℃. IL1β secreted into the medium was determined by ELISA. Data for healthy donors and PIGA-PNH were shown as mean +/- SD. Cells from three patients with PIGA-PNH (PIGA-PNH4-6) secreted very low levels of IL1β (403+/-326 pg/ml) after stimulation of NLRP3-inflammasomes with Pam_3CSK4 and ATP under these strong conditions. In contrast, cells from PIGT-PNH J1 secreted IL1β at a high level (25,000 pg/ml) that is higher than levels from three healthy donors (6,693+/-1,711 pg/ml). Similar results were obtained by stimulation with Pam_3CSK4 and MSU instead of ATP. Moreover, similar results were obtained by stimulation with LTA plus ATP or MSU.

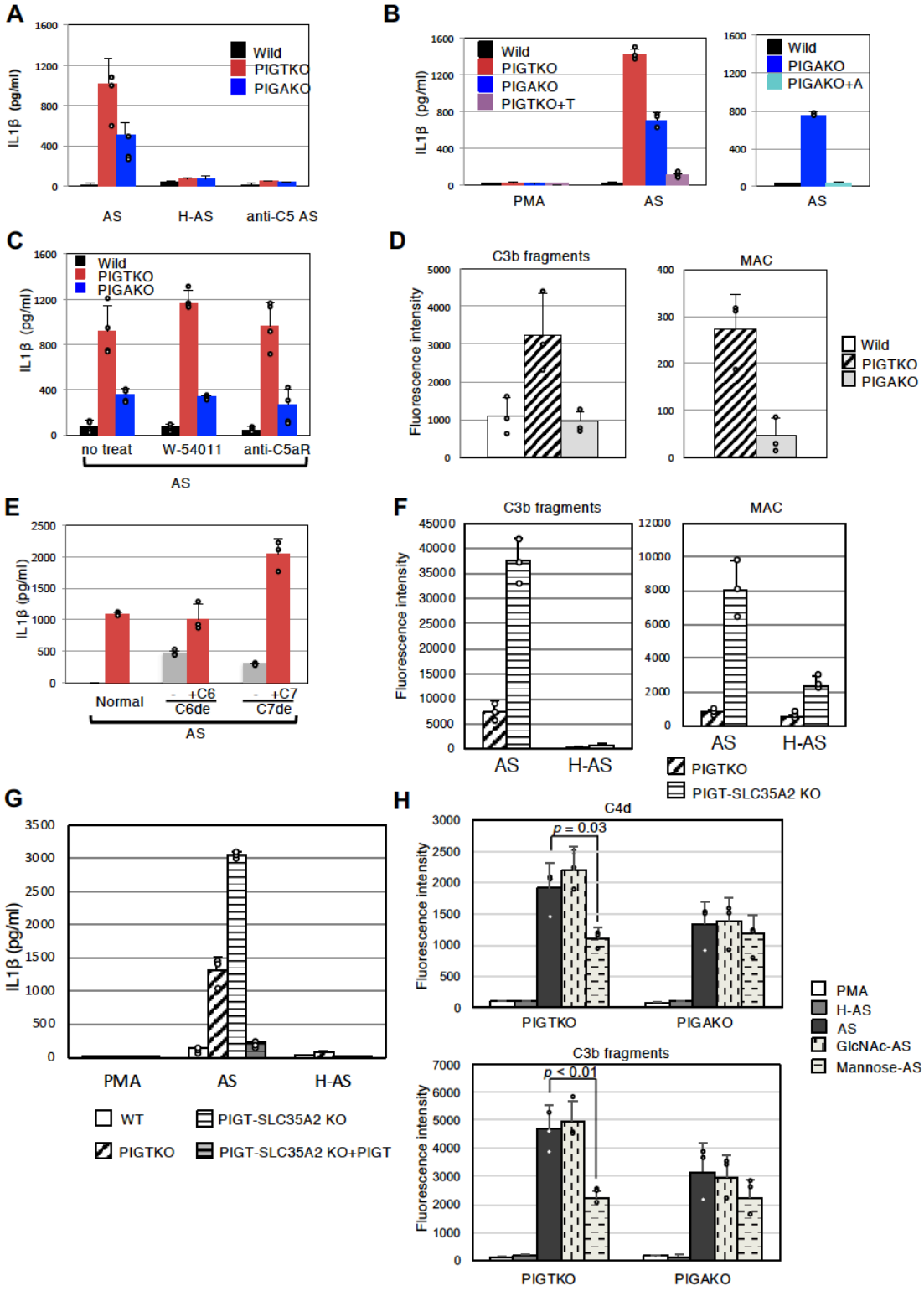

Figure 5. IL1β secretion from PIGT- and PIGA-defective THP-1 cells. A. Complement-mediated IL1β secretion from THP-1-derived macrophages. WT, PIGTKO and PIGAKO cells were incubated with acidified serum (AS), heat-inactivated AS (H-AS), or AS containing anti-C5 mAb. Supernatant

samples were collected after 5-hr incubation and analyzed for IL1β by ELISA. Mean + SD of three independent experiments. **B**. Reductions of IL1β secretion by transfection of *PIGT* and *PIGA* cDNAs into PIGTKO and PIGAKO cells (PIGTKO+T and PIGAKO+A, respectively). Cells differentiated by PMA were either left untreated (PMA) or incubated with AS (AS) under similar conditions as described in **A** and supernatants analyzed for IL1β. Mean + SD of three independent experiments. **C**. Effect of inhibiting C5aR on IL1β secretion from THP-1-derived macrophages. Cells were incubated with AS alone (no treat), or AS containing C5aR antagonist (W-54011) or anti-C5aR mAb. Supernatant was collected after 5 hr and analyzed for IL1β by ELISA. Mean + SD of duplicate samples from two independent experiments. **D**. Detection of C3b fragments (left) and MAC (right) by flow cytometry on PMA-differentiated THP-1 macrophages after incubation with AS. Geometric mean fluorescence intensity of medium-treated cells was subtracted from that of AS-treated cells. Mean + SD of three independent experiments. **E**. IL1β secretion from PIGTKO THP-1 macrophages stimulated with C6- or C7-depleted AS. PIGTKO THP-1 macrophages were incubated with AS, C6-depleted AS (-/C6de), C6de restored by C6 (+C6/C6de), C7-depleted AS (-/C7de), or C7de restored by C7 (+C7/C7de). Supernatant was collected after overnight incubation. Mean + SD of triplicate samples from two independent experiments (normal and C6-depleted sera) and one experiment (C7-depleted serum). **F**. Binding of C3b fragments (left) and MAC (right) on PIGTKO and PIGT-SLC35A2 double KO THP-1 macrophages after AS treatments. **G**. IL1β secretion from PIGTKO and PIGT-SLC35A2 double KO THP-1 macrophages after AS treatments. H. Binding of C4d (top) and C3b fragments (bottom) on PIGTKO and PIGAKO THP-1 macrophages after AS treatments and inhibition by mannose. Mean +SD of three independent experiments.

Table 1. Summary of clinical and genetic findings

	J1[A)]	G1[B)]	G2[C)]	G3[D)]
Age at diagnosis of PNH	68	49	65	66
Gender	Male	Female	Male	Male
Origin	Japanese	Caucasian	Caucasian	Caucasian
Signs and symptoms (age of onset)				
Urticaria	+ (30)[E)]	+ (26)		+ (48)
Arthralgia	+ (30)	+ (27)		+ (61)
Myalgia		+ (27)		+ (61)
Aseptic meningitis	+ (53)			+ (61)
Fever	+ (53)			+ (61)
Headache	+ (53)	+ [F)]		
Intravascular hemolysis	+ (67)	+ (44)[G)]	+	+ (61)[H)]
Abdominal pain		+ (39)		+ (61)
Ulcerative colitis		+ (52)[I)]		
Previous therapy	Corticosteroids Colchicine (for symptoms of autoinflammation)	Corticosteroids Diphenhydramine Cromoglycin Azathioprine (for symptoms of autoinflammation)	Corticosteroids (for residual hemolysis after start of eculizumab)	Corticosteroids Mycophenolate mofetil Dapsone Anakinra Canakinumab (for symptoms of autoinflammation)
Eculizumab	+ (69)	+ (52)	+ (66)	+ (66)

M[J)] allele of *PIGT*	c.250G>T[K)L)] (p.E84*)	c.1401-2A>G (exon 11 del)	c.761_764del GAAA[M)] (p.G254fs)	c.197delA[M)] (p.Y66fs)
P[J)] allele of *PIGT*	Entire deletion (18 Mb) [N)]	Entire deletion (8 Mb)	Entire deletion (12Mb) [M)N)]	Entire deletion (15 Mb) [M)]

A) J1 had recurrent urticaria and arthralgia since 30 years of age. At 53 years of age, he had first aseptic meningitis and since then had meningitis several times a year. A cerebrospinal fluid sample taken during an episode of meningitis had approximately 2,000 polymorphonuclear leukocytes per microliter. Since 58 years of age, frequencies of meningitis increased to twice a month. At 67 years of age, intravascular hemolysis was first noted. His white blood cell counts during asymptomatic period and after commencement of eculizumab therapy were within a normal range. Refer to Kawamoto M et al., *BMJ Case Rep*. 2018;2018 (8) for more detailed description of J1.

B) Refer to Supplemental Data in Krawitz PM et al., Blood 2013; 122:1312-1315 (7) for detailed description of G1.

C) 96% of granulocytes and 19% of erythrocytes of G2 were GPI-AP-defective. Additional diagnosis and symptoms: Arteriosclerosis with coronary heart disease, myocardial infarction (49 years) and recurrent left brain transient ischemic attacks (66 years), recurrent confusion symptoms, and disturbance of memory; cholecystectomy (43 years) in the following years remitting cholangitis; elevation of indirect bilirubin; B chronic lymphocytic leukemia (64 years), treatment with rituximab (Whether leukemic cells were from PNH clone was not known.); hemochromatosis (compound heterozygous), diagnosed at age of 66 because of elevation of ferritin, prostate adenoma. The patient died for cardiac decompensation with fulminant pulmonal edema and massive general arteriosclerosis with ulcerated plaques.

D) Additional diagnosis and symptoms of G3: Cholecystolithiasis (65 years); metabolic syndrome with obesity, diabetes and dyslipoproteinemia; sensorineural hearing loss (61 years); peripheral arterial occlusive disease; JAK2 V617F mutation (age of 66) (Whether the mutation occurred in PNH clone was not known.), neurinoma left side (52 years), increasingly personality changes and disturbance of memory since the beginning of the meningitis episodes until start of eculizumab.

E) Plus signs indicate presence of corresponding signs and symptoms. Numbers in parentheses indicate age when the symptom first recognized or eculizumab treatment started.

F) Headache often occurred associated with urticaria (first urticaria, followed by severe headache).

G) First time of significantly elevated lactate dehydrogenase (LDH)(7).

H) Patient reported on dark urine (panel d of Figure 1C).

I) G1 developed ulcerative colitis/proctitis about 5 years after diagnosis of PNH. Eculizumab was not effective to ulcerative colitis/proctitis in G1.

J) M, maternal; P, paternal.

K) Based on NM_015937.

L) The same variant c.250G>T in J1 (8) was found in two Japanese patients with inherited GPI deficiency (IGD) suffering from developmental delay, seizures and skeletal abnormality (Table S2)(11, 37).

M) Data are shown in Figure S2.

N) Deletions of J1 and G2 included entire *PIGU* gene as well as *PIGT*.

Table 2. Cytokines and other proteins in serum samples from G3, J1 and PIGA-PNH.

G3

Serum Samples in Figure1D	*1 Meningitis	*2 Meningitis	*3 Meningitis	*4 Meningitis	*5 Six months after start of eculizumab	Normal range
Thymidine kinase (U/L)	101	33.6	43.8	Not done	Normal	< 5
Soluble IL2-Receptor (U/ml)	1750	1345	3026	1237	Normal	158-635

J1

Serum Samples in Figure1D	*1 Interval	*2 Meningitis	*3 Hemolysis	*4 2.5 years after start of eculizumab	*5 3.5 years after start of eculizumab	*6 4.5 years after start of eculizumab	Normal range
IL18 (pg/ml)			1410	797	972	1150	<211.0
IL1 β (pg/ml)	0.291	＜0.125	4.670	<0.125	<0.125	<0.125	<0.928
IL1RA (pg/ml)	716	323	27500	239			85.6-660
IL6 (pg/ml)		127.0	4160	2.30	2.94	6.32	<2.410
Serum amyloid A (μ g/ml)	175.8	2433.0	282.6	＜2.5			<8.0
LDH (IU/L)	291	249	3004	157	165	169	120-250

IL1RA, IL1 receptor antagonist.

PIGA-PNH (4 patients without eculizumab therapy)

Patient	1	2	3	4	Normal range
IL18 (pg/ml)	288	289	263	443	<211.0
Serum amyloid A (μ g/ml)	5.0	7.1	6.8	8.3	<8.0
LDH (IU/L)	633	1190	923	1216	103-229